A Bond Graph Model for Object Grasping and Fingertip motion

Rashmi Arora, and Tarun Kumar Bera

Mechanical Engineering Department, Thapar University, Patiala, INDIA

***Abstract*:** *Usually industrial manipulators are of serial type but due to the drawback of small workspace, these are considered less useful as compared to parallel manipulators which have low accuracy. Hence hybrid manipulators solve these problems because they combine serial and parallel manipulators. In this paper, the model of a hybrid parallel-series manipulator is presented which serially connects two parallel manipulators. The bond graph models for forward and inverse dynamics are shown here. The objective of this paper is to track the trajectory by the thumb and index finger considering them as hybrid manipulators while grasping an object. Hence this hybrid manipulator can be used in multi fingered robotic grippers, pick and place operations and moving things etc. The simulation results and conclusions are shown in end which proves that within the acceptable limits, the command is followed by the response.*

Keywords: *hybrid manipulator, finger, bond graph, over whelming control.*

1. Introduction

Generally, industrial manipulators are serial manipulators having cantilever type structure with a large workspace but they have various drawbacks like low accuracy, low stiffness, and unwanted oscillations. Parallel manipulators have very high accuracy and high load to weight ratio but have a small workspace. So hybrid manipulators which are combination of both serial and parallel manipulators are considered. Hybrid manipulators presently are mainly of two types: the hybrid parallel-serial chain in which the parallel manipulators are connected in series and the hybrid series-parallel chain where parallel manipulators are connected in series by serial sub chains [1]. The human hand is an example of a hybrid manipulator in which there is a complex array of bones considered as links, joints, and a collection of parallel controlled actuators in the form of muscles and tendons that together, form a hybrid structure. Many researchers have developed hybrid mechanisms for the hand. Ramadan et al. [2] proposed a two-fingered hybrid manipulator hand where two 3-DOF parallel manipulators are connected in series. An inverse kinematics solution for the total mechanism was presented and CAD model was realized. Ramadan and Oohara [3] developed a chopstick like two fingered micromanipulator based on hybrid mechanism for 3-D manipulation of microscopic objects. It was made of two 3-prismatic-revolute-spherical parallel modules connected in series. A complete inverse kinematic analysis was done and optimization was carried out to maximize the reachable workspace of the end effector, based on which a CAD model was built. The model of a hybrid parallel-series manipulator is presented in this paper in which a one parallel manipulator having three DOF supports other parallel manipulator in series. The upper and lower platforms are connected by three prismatic legs of parallel manipulator. Each finger in a human hand can be considered as a hybrid manipulator where each phalanx is considered as a parallel manipulator and one phalanx is placed over other in series. Khurshid et al. [4] presented an approach to design an effective soft contact grasping system for a robotic gripper. It was concluded that the damping of soft finger, the stiffness of the spring in the soft finger and the friction between the soft contact surfaces effects considerably in manipulation of the object. A musculoskeletal model of the extensor mechanism of human finger was presented by Vaz and Singh [5] where dynamics of joints were analyzed. A compact system dynamics model for the hand prosthesis system was developed by Vaz and Hirai [6] from the word bond graph objects. Peerdeman et al. [7] described a three-dimensional hand prosthesis model based on the biomechanical structure of the human hand and demonstrated the correct operation of the finger underactuation, contact model and dynamic model. Lin et al. [8] presented an approach to model the hand configuration space directly. The analysis of local finger motions and constraints was done. The objective of this paper is to track the trajectory by the thumb and index finger considering them as hybrid manipulators while grasping an object. Hence this hybrid manipulator can be used in multi fingered robotic grippers, pick and place operations and moving things etc.

2. Model of Planar Hybrid Manipulator

2.1. Introduction

This model has two parallel manipulators connected in series. The joints are taken as pin joints and legs of the parallel manipulator are considered as prismatic pairs. The lower platform CE is fixed for the lower manipulator and upper platform AB has the movement. Three legs AC, AD and BE supports the moving platform and their lengths are L_1, L_2 and L_3 respectively. Point G is the centre of gravity and it is taken as the mid-point of line AB making an angle θ with the horizontal axis. For the upper manipulator, base CE is the moving platform AB of the lower manipulator. The velocity of point A in x-direction can be written as:

$$\dot{x}_a = \dot{x}_g + \dot{\theta}_g \, S_1 \sin\theta_g \tag{1}$$

where $(\dot{x}_g, \dot{y}_g)$ are the linear velocities of point G, $(\dot{\theta}_g)$ is the rotational velocity of G, S_1 is length of AG and S_2 is length of BG. Similarly, the velocity of point A in y-direction and linear velocities of point B can be written.

2.2. Bond Graph Model

Figure 1 shows the forward model named as plant model for the hybrid manipulator. The junctions $1_{\dot{x}_g}, 1_{\dot{y}_g}$ and $1_{\dot{\theta}_g}$ in the forward model represent the velocities $\dot{x}_g, \dot{y}_g$ and $\dot{\theta}_g$ respectively. Similarly other 1-junctions represent the velocities of other points. The mass (M_P) and the moment of inertia (J_P) of the platform are shown by the connections of 1-junctions with I-elements. The weight of the platform is modeled by connecting a source of effort with $1_{\dot{y}_g}$ junction. To modulate the transformer elements, flow sensors are added. The overwhelming controller gain is α_i and this is indicated by modulated source of effort element. All the joints connecting the three legs are frictionless joints. The junctions $1_{\dot{L}_1}, 1_{\dot{L}_2}$ and $1_{\dot{L}_3}$ represent the rate of change of leg length for three actuators. The equation for this is:

$$\dot{L}_1 = \mu_{X1}\left(\dot{x}_A - \dot{x}_C\right) + \mu_{Y1}\left(\dot{y}_A - \dot{y}_C\right) \tag{2}$$

where $\mu_{X1} = \frac{(x_A - x_C)}{L_1}$, $\mu_{Y1} = \frac{(y_A - y_C)}{L_1}$. Other leg lengths can be calculated in a similar manner.

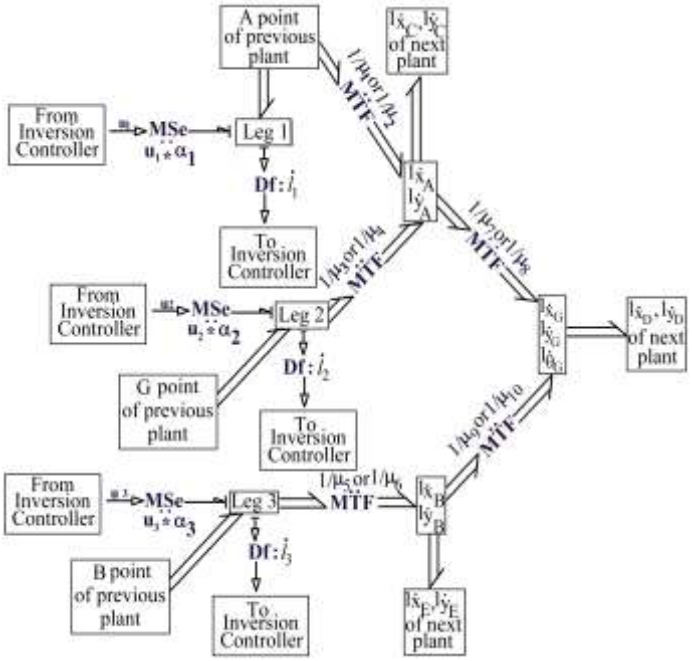

Fig. 1: Forward model (plant) for hybrid manipulator.

The commands given to the controller model are the reference positions (x_g, y_g, θ_g). For the lowermost manipulator, the flow inputs for the points C, D and E are zero as these are placed on the ground link which is

fixed. The inputs given to the plant model are the outputs coming from the controller model for three legs. The points C, D and E of the actuators for the upper plant are connected with the points A, G and B for the lower plant. To measure the deformation rate of the legs, three flow detectors are added to the 1-junctions.

3. Inverse Model of the Planar Hybrid Manipulator

The inverse dynamics or the controller model for the hybrid manipulator is made by having a mirror image of the forward model with some changes [**9**] as shown in Figure 2. Here positions (x_g, y_g, θ_g) are given as inputs and force applied in three legs of the manipulator is taken as output. Stiff spring-damper combinations are added in the model to remove the causal loops. Some I-elements had differential causality which is removed by adding some extra pad elements. The computation of final bond graph model is very easy.

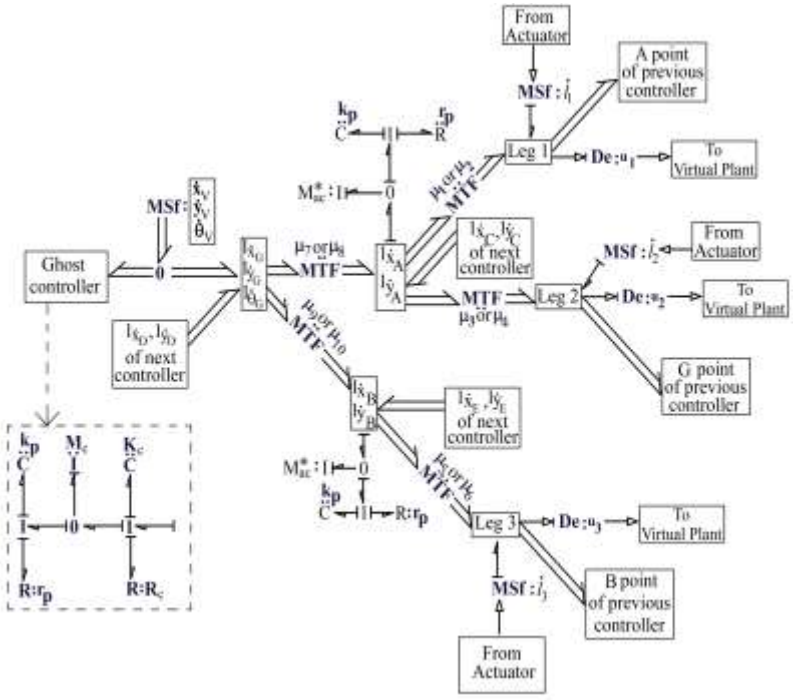

Fig. 2: Inverse model (controller) for hybrid manipulator.

4. Application of Hybrid Manipulator in Human Hand

The structure of a human hand is such that the thumb is located on one of the sides, parallel to the arm. The palm has five bones known as metacarpal bones. Human hands contain fourteen digital bones, also called phalanges, or phalanx bones: two in the thumb (the thumb has no middle phalanx) and three in each of the four fingers. These are the distal phalanx, carrying the nail, the middle phalanx, and the proximal phalanx. [**10**]. Each finger in a human hand can be considered as a hybrid manipulator where each phalanx is considered as a parallel manipulator and one phalanx is placed over other in series.

The various joints between these phalanges are shown in Figure 3. The movement of these joints for the thumb and index finger of the left hand in *x-y* plane is considered in this paper while grasping an object. The fingers gradually come closer to each other and finally, the smaller object is grasped by the finger.

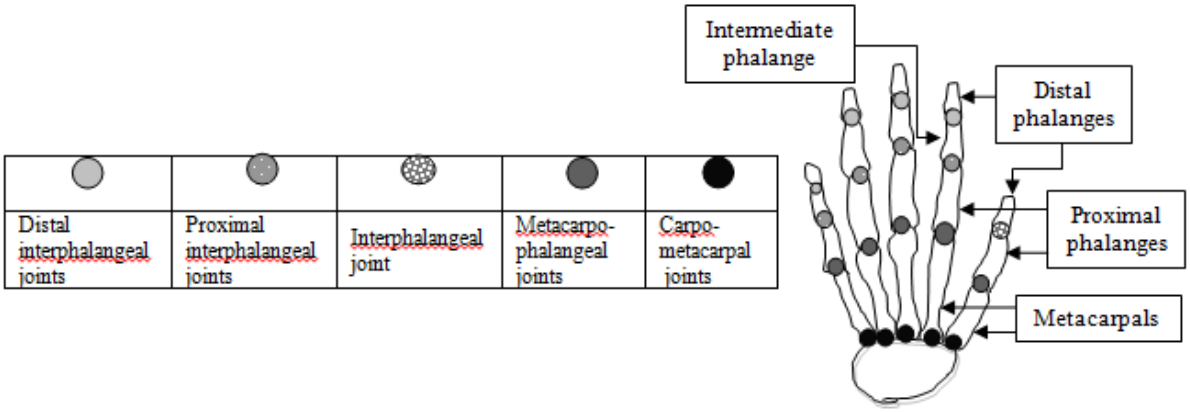

Fig. 3: Notations of various joints and their representation in human hand.

5. Simulation Results

Average weight of a joint in a finger is taken as 0.0125 kg [**11**]. Other parameters used in simulation are chosen suitably and are given in Table 1.

TABLE I Parameter values.

Sub systems	Parameter values			
Platform	$M_{\mathrm{P}} = 0.0125\,\mathrm{kg}$	$J_{\mathrm{P}} = 0.001\,\mathrm{kg\,m}^2$	$K_{\mathrm{j}} = 10^8\,\mathrm{N/m}$	$R_{\mathrm{j}} = 50\,\mathrm{Ns/m}$
Actuator	$k_{\mathrm{p}} = 10^8\,\mathrm{N/m}$	$r_{\mathrm{p}} = 50\,\mathrm{Ns/m}$		
Inverse system	$M^*_{\mathrm{P}} = 0.025\,\mathrm{kg}$	$J^*_{\mathrm{P}} = 0.025\,\mathrm{kg\,m}^2$	$M_{\mathrm{C}} = 3\,\mathrm{kg}$	$J_{\mathrm{C}} = 0.1\,\mathrm{kg\,m}^2$
	$K_{\mathrm{C}} = 10^4\,\mathrm{N/m}$	$R_{\mathrm{C}} = 1\,\mathrm{Ns/m}$	$\alpha = 100$	

The snap shots (camera- Sony-α 77, Japan) of eight different positions (only three positions are shown in Figure 4) for holding different chalk lengths in *x*-*y* plane were taken for the left hand for a time duration of 1.4 s. Different joints for the thumb and index finger were marked to note their positions. In this way, positions of centre of gravity for various joints for the thumb and index finger were noted down at different positions assuming the joint 1 as a fixed point. The *x* and *y* directions are shown in Figure 4 (a). Parallel spring damper combinations are attached with the tip of thumb and finger for grasping object effectively as shown in Figure 4 (a). The weight of the object i.e. chalk in this case acts in the downward direction and taken as 10 gms for the present case. The bond graph model for the same is shown in Figure 5 where weight of the object is taken into consideration in *y*-direction.

The X-ray photography was taken only for the chalk length of 1cm, 5cm and 8 cm as shown in Figure 6. The simulation of the system was performed for time duration of 1.4 s. The reference trajectories are the displacements of centroid of a joint in two directions i.e. *x* and *y* positions for various points. These reference positions of joints were fed to the inverse model. The motions from command points are compared with the corresponding motions obtained from response points for different positions of thumb and index finger obtained from simulation results.

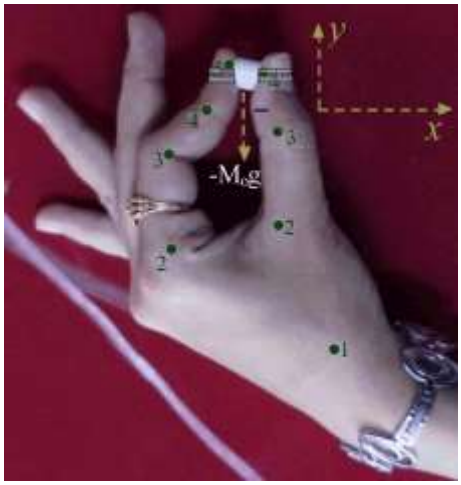

(a)

(b)

(c)

Fig. 4: (a) Final position of the finger, (b) Intermediate position of finger and (c) Initial position of finger.

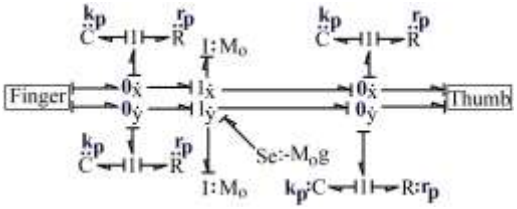

Fig. 5: A bond graph model for thumb and index finger grasping an object.

(a)

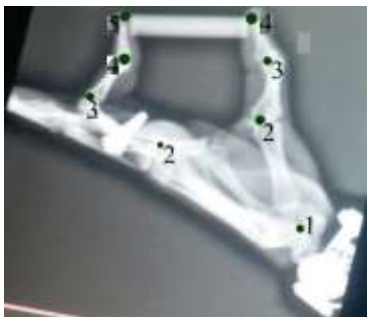

(b)

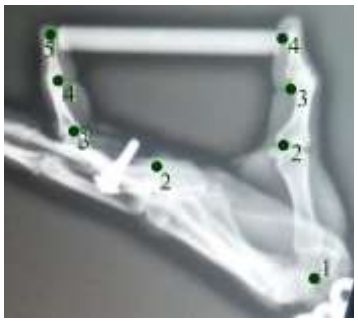

(c)

Fig. 6: (a) Final position, (b) Intermediate position and (c) Initial position of finger obtained from X-ray.

The initial conditions for different points of thumb and finger considered here are given in Table 2. The initial conditions are taken from the position with the biggest chalk length i.e. 8cm from X-ray (Figure 6(c)). The 1 point is considered as the origin of the coordinate axes.

Table II: Initial conditions (initial geometric configurations).

Thumb	Points	*x* (m)	*y* (m)	Thumb	Points	*x* (m)	*y* (m)
Metacarpal	A	0.002	0.04867	Proximal phalange	A	0.0062	0.06942
	G	0.00796	0.04867		G	0.01062	0.06942
	B	0.01392	0.04867		B	0.01501	0.06942
	C	0	0		C	0.002	0.04867
	D	0.004	0		D	0.00796	0.04867
	E	0.01592	0		E	0.01392	0.04867
Distal phalange	A	0.00318	0.08794				
	G	0.00752	0.08794				
	B	0.01186	0.08794				
	C	0.0062	0.06942				
	D	0.01062	0.06942				
	E	0.01501	0.06942				
Finger	Points	*x* (m)	*y* (m)	Finger	Points	*x* (m)	*y* (m)
Metacarpal	A	-0.01076	0.04088	Proximal phalange	A	-0.04052	0.05382
	G	-0.00638	0.04088		G	-0.03684	0.05382
	B	0.002	0.04088		B	-0.03316	0.05382
	C	-0.01276	0		C	-0.01076	0.04088
	D	-0.00876	0		D	-0.00638	0.04088
	E	0	0		E	0.002	0.04088
Intermediate phalange	A	-0.04584	0.0725	Distal phalange	A	-0.04741	0.08942
	G	-0.04276	0.0725		G	-0.04557	0.08942
	B	-0.03968	0.0725		B	-0.04373	0.08942
	C	-0.04052	0.05382		C	-0.04584	0.0725
	D	-0.03684	0.05382		D	-0.04276	0.0725
	E	-0.03316	0.05382		E	-0.03968	0.0725

The final result for trajectory tracking by the thumb is shown in Figure 7(a). Figure 7 (b) and (c) show the displacements of the object in y and x direction respectively. The velocity of the object in y-direction is shown in Figure 7(d). It can be easily seen that that the x-displacement for the tip of the thumb varies from 7.52 mm to -9.09 mm and y-displacement ranges from 87.94 mm to 94.69 mm. The displacement and velocity of the object is noted for 2 seconds. A small portion of the graph for 0.008 seconds is shown in Figure 7(c) and (d) to have a clear picture. Therefore, it is noted that the desired trajectory is tracked by the simulator for the thumb tip with minimal error. The commands fed to the inverse controllers are followed by the forward model for the controller gain of 100. If the controller gain is further increased, the error can be minimized.

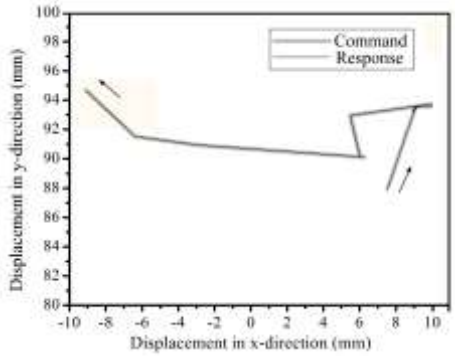

(a)

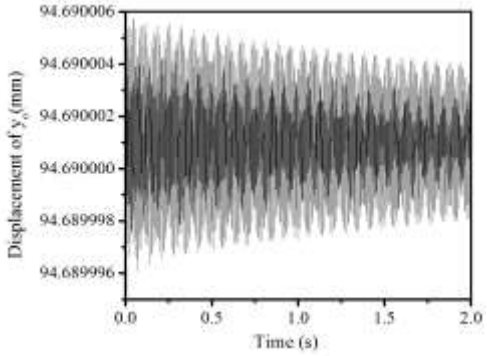

(b)

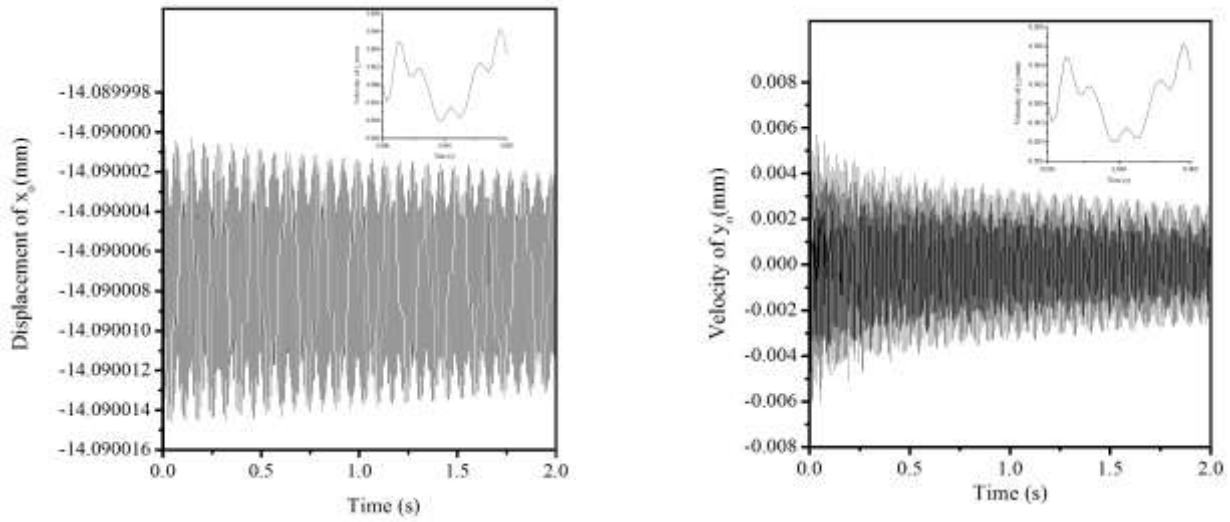

(c) (d)

Fig. 7: (a) Trajectory tracking for thumb in x-y plane, (b) y-displacement of the object, (c) x-displacement of the object and (d) velocity of the object in y-direction.

6. Conclusions

An example of thumb and finger in human hand is taken as a hybrid manipulator for which trajectory tracking was done for different phalangeal joints. Within the acceptable range, the command given to the controllers is followed by the response of the plants. With the increase in the gain of the overwhelming controller, the error limit can be decreased but the time taken by simulation is very large in that case.

7. References

[1] Kourosh Etemadi Zanganeh, "Kinematics of manipulators with parallelism, modularity and redundancy: analysis and design," PhD Dissertation, Montreal, Quebec, Canada, 1995.

[2] Ahmed A. Ramadan, Kenji Inoue, Tatsuo Arai, Tomohito Takubo and Izumi Hatta, "Micro-nano two-fingered hybrid manipulator hand," in *International Symposium on Micro-Nano Mechatronics and Human Sciences,* Nagoya, 2007, pp. 32-377.

http://dx.doi.org/10.1109/mhs.2007.4420822

[3] Ahmed A. Ramadan, Tomohito Takubo, Yasushi Mae, Kenichi Oohara and Tatsuo Arai, "Developmental process of a chopstick like hybrid structure two fingered micromanipulator hand for 3-D manipulation of microscopic objects," *IEEE Transactions on Industrial Electronics,* vol. 56 (4), pp. 1121-1135, 2009.

http://dx.doi.org/10.1109/TIE.2008.2008753

[4] http://cdn.intechopen.com/pdfs-wm/18895.pdf

[5] Anand Vaz and Kanwalpreet Singh, "A bond graph model for the extensor mechanism of human finger," in *Proc. NaCoMM*, 2009, pp. 139-145.

[6] http://www.researchgate.net/publication/242082279_Modeling_a_Hand_Prosthesis_with_Word_Bond_Graph_Objects

[7] Bart Peerdeman, Daphe Boere, Laura Kallenbergy Stefano Stramigioli and Sarthak Misra, "A biomechanical model for the development of myoelectric hand prosthesis control systems," in *32nd Annual International Conference of the IEEE EMBS Buenos Aires*, 2010, pp. 519-523.

http://dx.doi.org/10.1109/iembs.2010.5626085

[8] http://www.ifp.illinois.edu/~yingwu/papers/Humo00.pdf

[9] TK Bera, AK Samantaray and R. Karmakar, "Robust overwhelming control of a hydraulically driven three degrees of freedom parallel manipulator through a simplified fast inverse model," *Proceedings of the Institution of Mechanical Engineers, Part I: Journal of Systems and Control Engineering*, vol. 224(2), pp. 169-184, 2010.

http://dx.doi.org/10.1243/09596518JSCE828

[10] http://en.wikipedia.org/wiki/Finger

[11] *Anthropometry and Mass distribution for Human Analogues*, vol. 1, Military Male Aviators, Naval Biodynamics Laboratory, New Orleans, LA, 1988, pp. 37.

APPENDIX

Abbreviations

C	capacitance
De	effort detector
Df	flow detector
DOF	degrees of freedom
I	inertance
R	resistance
Se	source of effort
Sf	source of flow

Notation

J	polar Moment of Inertia (kg-m^2)
k, K	stiffness (N/m)
L_i	length of legs (m) (i = 1….3)
$\dot{L}_i$	rate of change of leg length of manipulator (m/s) (i = 1….3)
M	mass (kg)
r, R	damping
S_1	length of platform *ag* of hybrid manipulator (m)
S_2	length of platform *gb* of hybrid manipulator (m)
t	time
V_{ref}	reference velocity
x , y	displacement in the x and y direction respectively (m)
$\dot{x}$, $\dot{y}$	velocity in x and y direction (m/s)
α_i	controller gain
θ	rotation about the z-axis
$\dot{\theta}$	angular velocity about z-axis (rad/s)
μ	transformer modulus
ω	angular velocity (rad/s)

Subscripts

C	controller
g	centre of gravity
o	object
p	pad
P	plant

Superscript

*	an estimate (virtual)